

β -TRICALCIUM PHOSPHATE DOPED WITH Ga^{3+} FOR BONE SUBSTITUTION: SYNTHESIS AND BIOLOGICAL PROPERTIES

Ioana-Sandra SERDARU¹, Nicoleta-Laura DRAGOMIR¹, Cristina-Daniela GHÎȚULICĂ¹, Adrian-Ionuț NICOARĂ^{1,2}, Georgeta VOICU¹, Andreia CUCURUZ^{3*}, Florin IORDACHE⁴

This study explores the synthesis and characterization of β -tricalcium phosphate (β -TCP) and β -TCP doped with 0.5% Ga^{3+} for regenerative medicine applications. Precursor powders, obtained via co-precipitation, were thermally treated at 1150°C to form ceramic masses. XRD, Raman spectroscopy, and SEM-EDX analyses confirmed Ga^{3+} substitution in the calcium phosphate network, leading to structural and spectral modifications. Ga^{3+} doping resulted in a β -TCP+TTCP (tetracalcium phosphate) mixture, enhancing cell adhesion, proliferation, and reducing oxidative stress. The findings suggest that Ga^{3+} -doped β -TCP ceramics offer promising properties for biomedical applications.

Keywords: β -TCP (beta-tricalcium phosphate), Gallium dopant, coprecipitation, regenerative bone tissue

1. Introduction

Bioceramics have become essential in medicine, especially for treating and restoring the functions of hard tissues. With a varied composition, they are highly versatile and have numerous applications in medicine and biotechnology, particularly in dental and orthopedic fields. They can be presented in both dense and porous forms, with densities similar to those of hard tissues, offering appropriate mechanical and biological behavior for their intended functions. As a result, bioceramics can provide long-term durability and stimulate bone growth

¹ Department of Science and Engineering of Oxide Materials and Nanomaterials, Faculty of Chemical Engineering and Biotechnologies, National University of Science and Technology POLITEHNICA Bucharest, Romania

² National Research Center for Micro and Nanomaterials, Faculty of Applied Chemistry and Materials Science, University POLITEHNICA of Bucharest, Romania

³ Department of Biomaterials and Medical Devices, Faculty of Medical Engineering, National University of Science and Technology POLITEHNICA Bucharest, Romania, *Correspondence: andreia.cucuruz@upb.ro

⁴ Department of Preclinical Sciences, Faculty of Veterinary Medicine, University of Agronomic Sciences and Veterinary Medicine of Bucharest, Romania

and regeneration by promoting osteoblast adhesion and vascularization, making them ideal for use in implantology and tissue regeneration [1-6].

The predominant calcium phosphates in medical applications are tricalcium phosphate and hydroxyapatite. Future studies have continued to explore the benefits of amorphous calcium phosphate, octacalcium phosphate, anhydrous dicalcium phosphate, and dibasic phosphate in tissue engineering applications [5].

Hydroxyapatite (HAp) is the most widespread crystalline mineral phase in hard tissue, representing approximately half part of the bone tissue, almost 70% of the dry weight. The chemical formula for HAp is $\text{Ca}_5(\text{PO}_4)_3(\text{OH})$, but it is often written as $\text{Ca}_{10}(\text{PO}_4)_6(\text{OH})_2$ to highlight its hexagonal structure. HAp is considered a promising biomaterial due to its chemical similarity to human hard tissues, demonstrating excellent biocompatibility, osteoconductivity, and bioactivity. This means that it can stimulate new bone formation, with a huge proliferation and differentiation of osteoblasts. HAp has been used in a variety of medical applications, such as drug delivery systems, orthopedic and dental implants, and as filler material in reconstructive surgery [1, 5, 6].

Octacalcium phosphate (OCP), as a precursor to hydroxyapatite crystals (HAp), along with amorphous calcium phosphate (ACP) and dicalcium phosphate dihydrate (DCPD), plays a significant role in bone formation and biominerization. While it has a structure similar to HAp, OCP is more unstable and gradually hydrolyzes into HAp at physiological pH. OCP can exhibit variations in stoichiometry (Ca/P) and is commonly used in bone regeneration research. OCP is known for its osteoinductive properties and is used in metal graft coatings, composite scaffolds for bone reconstruction, and other surgical applications for bone regeneration. Therefore, the use of OCP in biomaterials for bone regeneration has promising potential, and investigating its biological mechanism and the impact of its structural variations on biological activity is essential for the development of future bone therapies [5].

Two polymorphic crystalline forms of tricalcium phosphate (TCP) are known: α -TCP with a hexagonal structure and β -TCP with an orthorhombic structure. β -TCP exhibits a highly stable phase, allowing for long-term storage at room temperature in a dry environment, which makes it more stable than α -TCP. Osteoconductivity and osteoinductivity are determinants for β -TCP in clinical applications compared with HAp, mainly used in bone cements and bioceramics. On the other hand, α -TCP is commonly used in cements due to its ability to change the crystalline phase to hydroxyapatite (HAp) upon contact with water. It is important to note that pure α -TCP has a high resorption rate, which means that the resorption process can outpace new bone formation, potentially causing a desynchronization between bone regeneration and implant degradation. As a result, α -TCP is typically employed as a component in phosphate cements alongside other phosphate-based materials. In contrast, β -TCP exhibits a

decreasing resorption rate than α -TCP and demonstrates greater potential for bone regeneration.

Although β -TCP offers advantages such as enhanced osteoconductivity and superior biodegradability compared to other materials, its relatively low mechanical strength makes it suitable as a bone substitute only when combined with other materials, such as hydroxyapatite. Consequently, it is often combined with HAp in commercial products, resulting in biphasic products with significant applications in bone regeneration and orthopedics [2, 4, 5].

A modern strategy, essential in regenerative medicine and tissue engineering, is the doping of bioceramics based on phosphate phases with various ions. This technique allows for the enhancement of material properties, such as biocompatibility, osteoconductivity and resistance to bacteria, thereby expanding their application in the treatment and regeneration of bone tissue. For example, metal ions such as silver (Ag^{2+}), copper (Cu^{2+}), strontium (Sr^{2+}), zinc (Zn^{2+}), and magnesium (Mg^{2+}) are considered essential trace elements for bone growth and mineralization and have demonstrated significant antibacterial and anti-inflammatory effects [4, 7-9].

Recently, doping calcium phosphates with Ga^{3+} has been investigated, and it has been shown that Ga^{3+} induces an efficient antibacterial and anti-inflammatory effect while promoting bone regeneration without causing cytotoxicity [7, 9, 10]. Therefore, Ga^{3+} -doped apatites have demonstrated antibacterial effects both *in vivo* and *in vitro*. Moreover, Ga^{3+} has an effect on inhibits bone resorption, primarily being used in biomedical applications. Additionally, Ga^{3+} exhibits remarkable antibacterial activity and is believed to play an essential role in the acceptance of orthopedic implants [4, 7, 8, 10].

There have also been extensive studies on Ga^{3+} -doped bioglass, including phosphate types, demonstrating its effectiveness in terms of biological behavior (e.g., osteogenic, antibacterial, anti-inflammatory, angiogenic effects) [9, 11, 12]. As a result, gallium and calcium phosphates have garnered significant attention from the scientific and medical communities due to their unique properties and potential in regenerative medicine and orthopedics. This study aims to synthesize and characterize the morphological, structural, and biological properties of Ga^{3+} -doped β -TCP with potential applications in regenerative medicine.

2. Materials and methods

The ceramic masses based on β -tricalcium phosphate (β -TCP) both undoped and doped with 0.5 mol% Ga^{3+} , was synthesized using the co-precipitation method and the predefined precursor – Fig. 1. Chemically pure raw materials were used: calcium nitrate tetrahydrate ($\text{Ca}(\text{NO}_3)_2 \cdot 4\text{H}_2\text{O}$, Sigma Aldrich), ammonium phosphate ($(\text{NH}_4)_2(\text{HPO}_4)$, Sigma Aldrich), gallium oxide

(Ga_2O_3 , Sigma Aldrich), hydrochloric acid (HCl, 36.5%, Sigma Aldrich), and ammonium hydroxide (NH_4OH , Sigma Aldrich). Distilled water was used as the solvent. The raw materials were dosed at a molar ratio of $\text{CaO}:\text{P}_2\text{O}_5$ (Ga_2O_3) of 3:1 (0.5).

The two salts, $\text{Ca}(\text{NO}_3)_2 \cdot 4\text{H}_2\text{O}$ and $(\text{NH}_4)_2(\text{HPO}_4)$, were dissolved separately in a minimal amount of water by continuous magnetic stirring at 80°C, yielding two clear solutions. Separately, the required amount of Ga_2O_3 was dissolved in HCl solution by magnetic stirring at 60°C until a clear solution was obtained, which was then added to the aqueous solution of $\text{Ca}(\text{NO}_3)_2$. The aqueous solution of $(\text{NH}_4)_2(\text{HPO}_4)$ was added dropwise for 2 hours at 80°C, ensuring that the pH was continuously adjusted to approximately 9 (10) by adding NH_4OH . The obtained precipitates, with and without Ga^{3+} , were left to mature for 48 hours at room temperature, after which they were washed until the pH was approximately 7, and then dried in an oven at 80°C for 48 hours. After drying, the precipitates were mortar ground and sieved, resulting in precursor powders of TCP, which were later dried, uniaxially pressed (cylindrical specimens, approximately 7 mm in diameter, 2 mm in height), and heat-treated at 1150°C for 3 hours.

To characterize the precursor powders and the synthesized ceramic masses, different characterization techniques were used.

Thus, the chemical-mineralogical composition of these materials was evaluated by X-ray diffraction (XRD, Shimadzu XRD 6000 diffractometer, Shimadzu, Kyoto, Japan), with Ni-filtered $\text{Cu K}\alpha$ radiation ($\lambda = 1.5406 \text{ \AA}$), in the 2θ range of 5 to 65°, a scanning speed of 2°/min, and a step size of 0.02 min/step. To demonstrate doping of the calcium phosphate network with 0.5 mol% Ga^{3+} , Raman spectroscopy was also used in addition to XRD. This was performed with a Horiba JobinYvon LabRam HR spectrometer, in the range of 0–1200 cm^{-1} , using the green line of an Ar laser ($\lambda = 514 \text{ nm}$).

Scanning electron microscopy (Quanta Inspect F50 FEG) electron microscope with a resolution of 1.2 nm, Thermo Fisher, Eindhoven, Netherlands), and for electron beam conductivity enhancement, they were coated with a thin gold layer to emphasize the morpho-structural characterization of obtained materials.

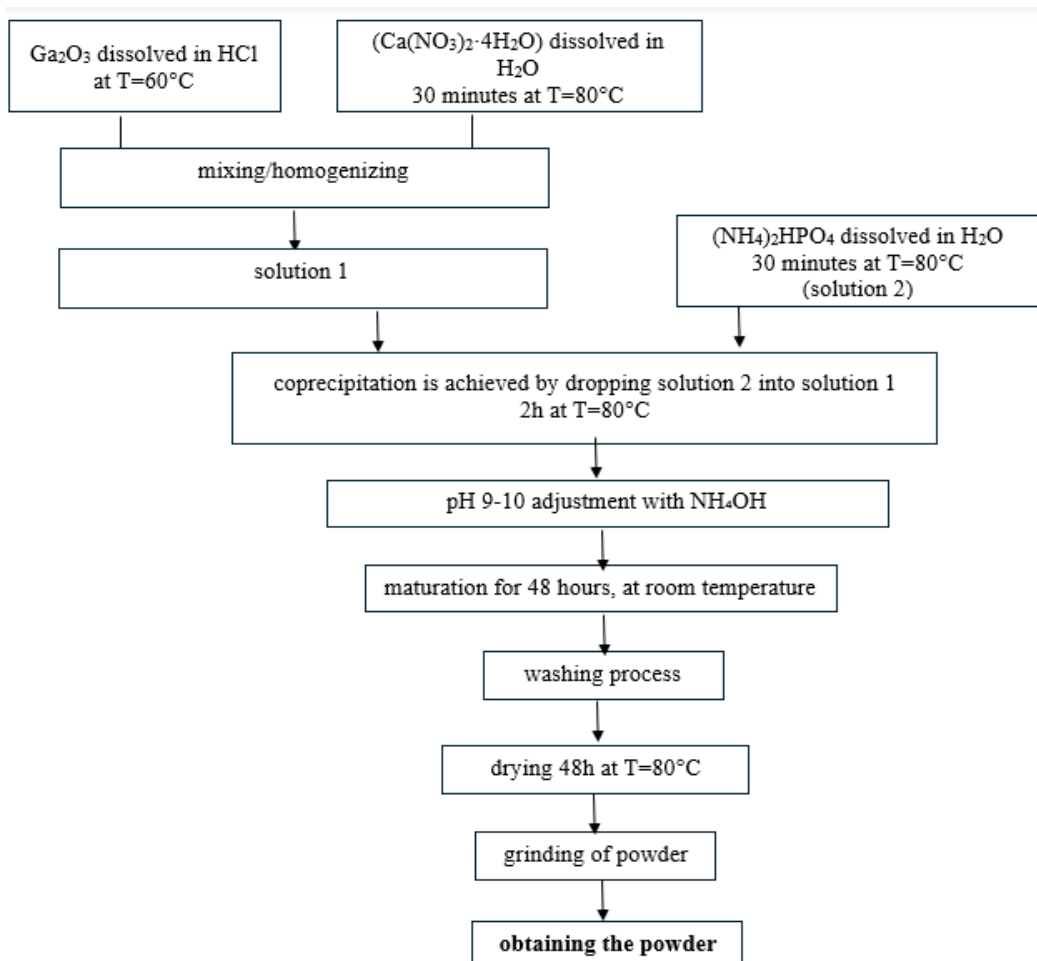


Fig. 1. Scheme for obtaining the precursor powder of β -TCP with/without 0.5% Ga^{3+}

The MTT assay and fluorescence microscopy for monitoring live cells were used to assess the in vitro biocompatibility of the samples. Each test was performed in triplicate using AFSC cells (amniotic fluid-derived mesenchymal stem cells).

About the cell proliferation, viability, and cytotoxicity in the MTT assay, we used a colorimetric quantitative method. Its aim is the reduction of a yellow tetrazolium salt, MTT (3-(4,5-dimethylthiazol-2-yl)-2,5-diphenyl tetrazolium bromide), to dark blue formazan. The reduction is catalyzed by mitochondrial enzymes, primarily succinate dehydrogenase, serving as an indicator of cell and mitochondrial integrity. The insoluble formazan can be dissolved using isopropanol, dimethyl sulfoxide, or another organic solvent. Spectrophotometric evaluation then measures the optical density (OD), which correlates absorbance with dye concentration and the number of metabolically active cells in the culture.

Cells were cultured in 96-well plates at a seeding density of 3000 cells per well under different experimental conditions. Then, 10 μ L of 12 mM MTT solution was added and incubated at 37°C for 4 hours. Subsequently, 100 μ L of SDS-HCl solution was added, and the solution was vigorously pipetted to dissolve the formazan crystals. The plates were incubated for 1 hour, followed by pipetting to homogenize the solution and remove bubbles to avoid interference with the absorbance reading. The optical density was measured at 570 nm using a spectrophotometer (TECAN, Männedorf, Switzerland).

Fluorescence microscopy was used to evaluate the biocompatibility of the ceramic masses by monitoring live cells with the fluorophore RED CMTPX (Life Technologies, Invitrogen, Carlsbad, CA, USA). CMTPX was added after 48 hours of cell cultivation in contact with the ceramics to assess the viability and morphology of mesenchymal stem cells. The fluorophore was added to the culture medium at a final concentration of 5 μ M, and cells were incubated for 30 minutes to allow dye penetration. In the final step, the cells were washed with PBS and then visualized by fluorescence microscopy. Photomicrographs were taken with a digital camera controlled by Axio-Vision 4.6 software (Carl Zeiss, Jena, Germany). Control cells consisted of mesenchymal stem cells cultured in the same medium but without ceramic materials.

The oxidative stress induced by the presence of the ceramic substrate, was observed using the AFSC cells were first seeded at a density of 3000 cells in 300 μ L of DMEM culture medium supplemented with 10% fetal bovine serum and 1% antibiotics (penicillin, streptomycin/neomycin) in 96-well plates. After 24 hours of seeding, the cells were exposed to ceramic materials. After 24 hours, cell viability was assessed at multiple time intervals. Oxidative stress was evaluated using the GSH-Glo™ Glutathione Assay kit. This kit measures the amount of glutathione, an antioxidant agent. The glutathione produced by the cells is converted by glutathione S-transferase into oxidized glutathione, and the amount of glutathione produced is directly proportional to the amount of glutathione S-transferase that transforms a substrate that does not emit light into one that emits light. The more intense the light, the more glutathione S-transferase has been used, indicating more glutathione has been synthesized, and thus the cell has been under more stress. The protocol consisted of adding 100 μ L of 1X GSH-Glo™ Reagent and incubating at 37°C for 30 minutes. Then, 100 μ L of Luciferin Detection Reagent was added and incubated at 37°C for another 15 minutes. After 15 minutes, the plate was well mixed, and the plate was read on a luminometer.

3. Results and discussions

From the diffraction patterns of the β -TCP precursor powders, either undoped or doped with 0.5% Ga^{3+} , shown in Fig. 2, it can be observed that

hydroxyapatite (HAp, JPCDS 084-1998) is identified as the unique phase. Furthermore, it can be seen that doping with 0.5% Ga^{3+} causes a shift in the diffraction peaks characteristic of HAp, suggesting that Ga^{3+} has entered its structure.

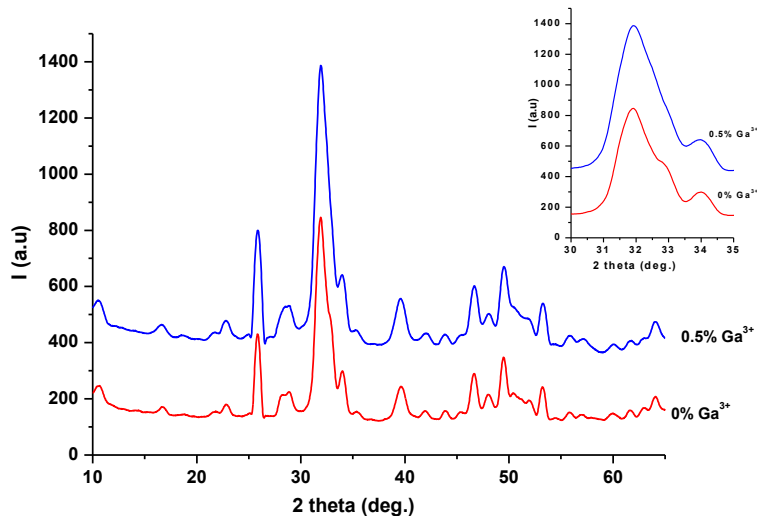
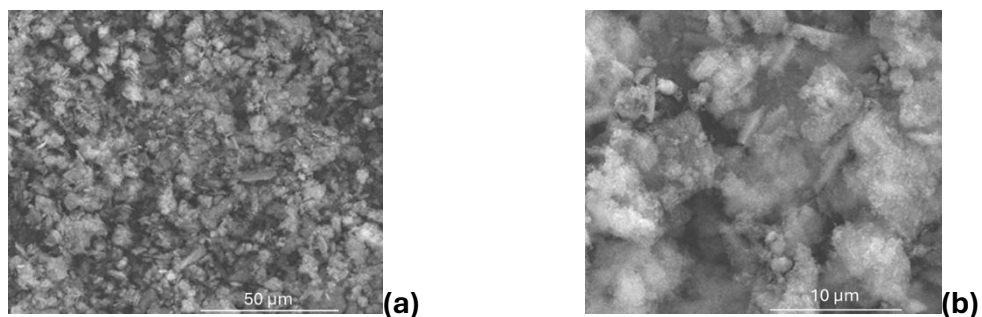


Fig. 2. X-ray patterns for undoped and doped precursor powders

Moreover, the scanning electron microscopy (SEM) images of the precursor powder doped with 0.5% Ga^{3+} (Fig. 3) show morphologies typical for apatite phases, specifically nanometric quasi-spherical particles organized into agglomerates or aggregates, and very thin rods or plates. The EDX spectrum demonstrates the presence of Ca, P, O, and Ga in the composition.



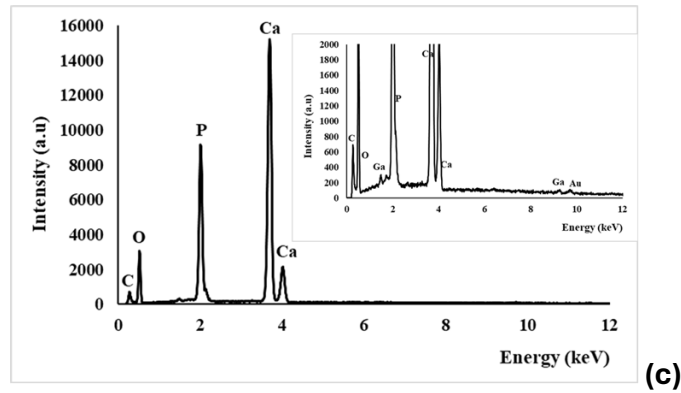
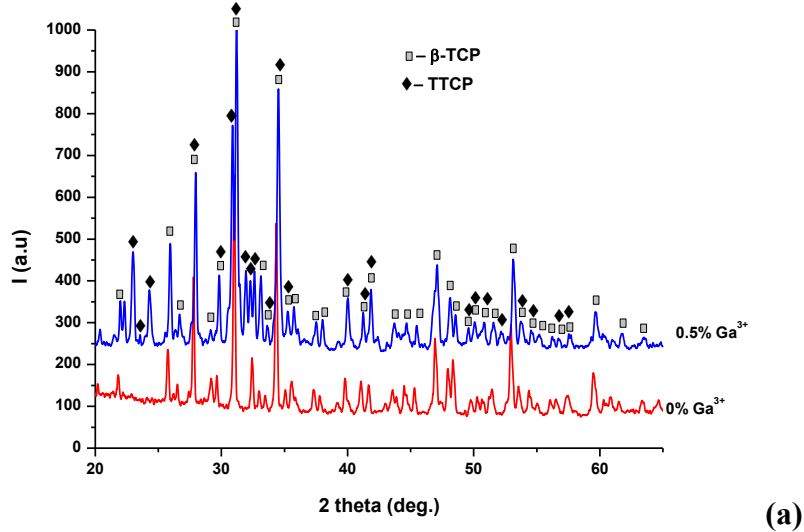


Fig. 3. Scanning electron microscopy (SEM) images of the β -TCP/Ga precursor powder

By performing thermal treatment at 1150°C for 3 hours on the samples made from the precursor powders, X-ray diffraction (Fig. 4a) shows that for the undoped sample, β -TCP (JCPDS 009-0169) forms as the unique phase, while for the doped sample, in addition to the predominant β -TCP phase, tetracalcium phosphate (TTCP, JCPDS 070-1379) is also favored. Additionally, Raman data (Fig. 4b) closely correlate with these XRD results, showing that for the 0.5% Ga^{3+} -doped sample, the intensities of the characteristic absorption bands for the undoped sample (430 cm^{-1} , 582 cm^{-1} , 959 cm^{-1} , 1042 cm^{-1}) increase and shift, while new absorption bands (287 cm^{-1} , 604 cm^{-1} , 1118 cm^{-1}) appear. This occurs as a result of the effects due to Ga^{3+} ions substitution in the lattice, such as changes in the Ca-O bonds or new vibrational modes.



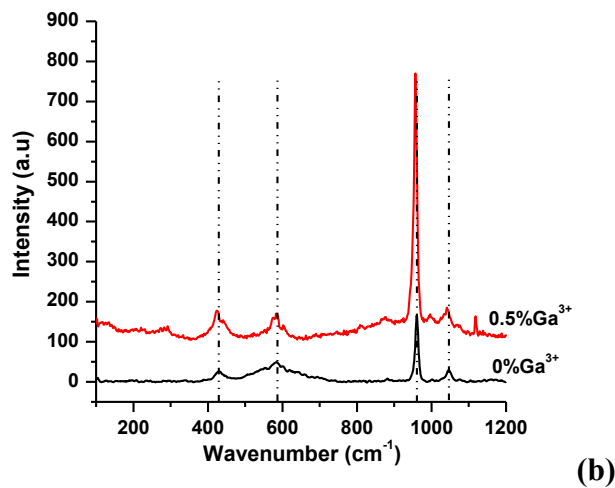


Fig. 4. X-ray patterns (a) and Raman spectra (b) for undoped and doped powders, thermally treated at 1150°C for 3 hours.

Also, from Fig. 5, both for the undoped mass and the 0.5% Ga^{3+} -doped mass, the SEM images highlight predominantly elongated quasi-spherical particles, typical of the β -TCP phase. Additionally, for the doped sample, polyhedral particles, characteristic of TTCP, are also observed.

From a biological behavior perspective for the synthesized ceramic masses, the data obtained are summarized in Fig. 6, providing information on cytotoxicity (cell adhesion and proliferation) and oxidative stress on cells that these ceramics may exert. It can be observed that for both undoped and 0.5% Ga^{3+} -doped β -TCP-based ceramic masses, not only do the cells proliferate (Fig. 6a, b), but this process is not accompanied by an increase in oxidative stress, as shown by the GSH test (Fig. 6c).

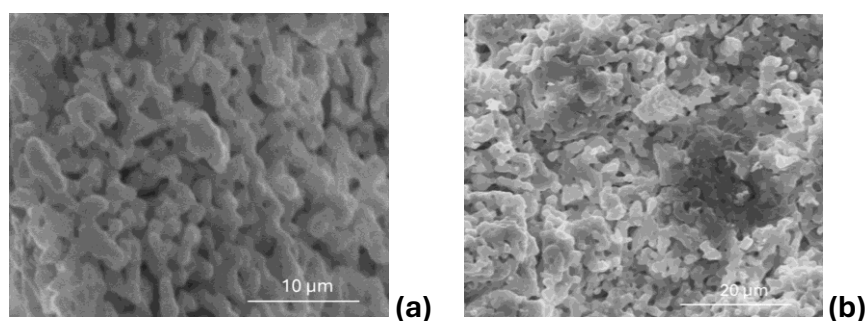


Fig. 5. Scanning electron microscopy (SEM) images for β -TCP-based ceramic masses thermally treated at 1150°C for 3 hours: a- undoped and b- doped with 0.5% Ga^{3+} .

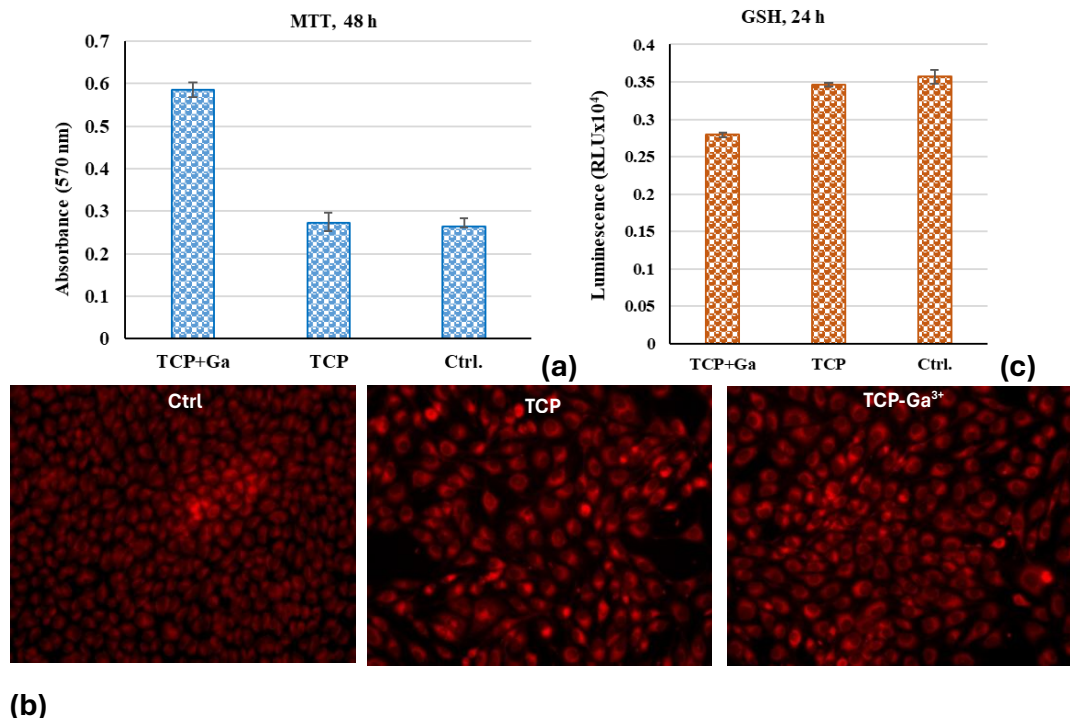


Fig. 6. In-vitro evaluation of the biological behavior of undoped and 0.5% Ga^{3+} -doped β -TCP based ceramic masses, thermally treated at 1150°C for 3 hours: a- MTT test (3-(4,5-dimethylthiazolium)-2,5-diphenyl tetrazolium bromide); b- images obtained by optical fluorescence microscopy ($\times 20$) associated with the MTT test; c- oxidative stress (GSH).

Furthermore, the results at 24 hours indicate a significant decrease in the intracellular glutathione level for the ceramic masses compared to the control, meaning fewer free radicals were produced in the cells. Also, the ceramic mass doped with 0.5% Ga^{3+} induced a significantly lower GSH level compared to the undoped one. Thus, it can be stated that the presence of these ceramic masses led to greater cell viability without increasing intracellular oxidative stress.

4. Conclusions

From the study conducted, it was shown by XRD that the precursor powders obtained by the coprecipitation method for producing β -TCP-based ceramic masses, both undoped and doped with 0.5 mol% Ga^{3+} , are composed of hydroxyapatite as the unique mineral phase. The shift in the maximum diffraction peaks in the doped mass demonstrates the substitution of Ga^{3+} in the HAp structure.

By thermal treatment at 1150°C for 3 hours, doping leads to the formation of a mixture of calcium phosphates, namely β -TCP and TTCP, unlike the undoped

mass, where only β -TCP was identified as the unique phase. In the future, for the doped sample, to achieve β -TCP as the unique phase, it is recommended to perform thermal treatment below 1150°C for 3 hours.

Additionally, in the case of Ga^{3+} doping, the shift in the maximum diffraction peaks in the ceramic mass diffraction pattern demonstrates Ga^{3+} substitution in the calcium phosphate network. Furthermore, the Raman spectrum of the 0.5% Ga^{3+} -doped ceramic mass, compared to the undoped sample, shows shifts and intensity changes in the absorption bands, as well as the appearance of new absorption bands. These changes occurred as a result of the effects of Ga^{3+} ions substitution in the lattice, such as modifications in the Ca-O bonds or new vibrational modes.

The conclusion of this study indicates that the 0.5% Ga^{3+} -doped β -TCP ceramic mass exhibits significantly better cell adhesion and proliferation than the undoped one and also induces much lower oxidative stress. Therefore, β -TCP ceramics doped with 0.5% Ga^{3+} can be considered suitable for current applications in regenerative medicine.

Acknowledgement

The authors are grateful to the Romanian Government for providing access to the research infrastructure of the National Centre for Micro and Nanomaterials through the National Program titled “Installations and Strategic Objectives of National Interest”.

R E F E R E N C E S

- [1] *Vaiani, Lorenzo, et al.*, "Ceramic Materials for Biomedical Applications: An Overview on Properties and Fabrication Processes." *J. Funct. Biomater.* 2023, 14, 146. <https://doi.org/10.3390/jfb14030146>.
- [2] *Sergey V. Dorozhkin.*, "Current State of Bioceramics." *Journal of Ceramic Science and Technology* Vol. 9, No. 4.
- [3] *Harshavardhan Budharaju a,1 , Shruthy Suresh a,1 , Muthu Parkkavi Sekar a , Brigita De Vega b , Swaminathan Sethuraman a , Dhakshinamoorthy Sundaramurthi a,11 , Deepak M. Kalaskar b,11 H. Budharaju, S. Suresh, M.P. Sekar et al.*, "Ceramic materials for 3D printing of biomimetic bone scaffolds – Current state-of-the-art & future perspectives"; *Materials & Design* 231 (2023) 112064
- [4] *Pawel Dec , Andrzej Modrzejewski, Andrzej Pawlik*, "Existing and Novel Biomaterials for Bone Tissue Engineering", *Int. J. Mol. Sci.* 2023, 24, 529. <https://doi.org/10.3390/ijms24010529>
- [5] *Hou, Xiaodong, et al.*, "Calcium Phosphate-Based Biomaterials for Bone Repair." *J. Funct. Biomater.* 2022, 13, 187, <https://doi.org/10.3390/jfb13040187>.
- [6] *Harshavardhan Budharaju, Shruthy Suresh, Muthu Parkkavi Sekar, Brigita De Vega, Swaminathan Sethuraman, Dhakshinamoorthy Sundaramurthi, Deepak M. Kalaskar,*"Ceramic materials for 3D printing of biomimetic bone scaffolds – Current state-of-the-art & future perspectives", *Materials & Design* 231 (2023) 112064, <https://doi.org/10.1016/j.matdes.2023.112064>

- [7] *Saravanakumar Ponnusamy, Ramya Subramani, Shinyjoy Elangomannan, Kavitha Louis, Manoravi Periasamy, and Gopi Dhanaraj*, "Novel Strategy for Gallium-Substituted Hydroxyapatite/Pergularia daemia Fiber Extract/Poly(N-vinylcarbazole) Biocomposite Coating on Titanium for Biomedical Applications", *ACS Omega* 2021, 6, 22537–22550, <https://doi.org/10.1021/acsomega.1c02186>
- [8] *Wei Shuai, Jianguo Zhou, Chen Xia, Sirui Huang, Jie Yang, Lin Liu, Hui Yang*, "Gallium-Doped Hydroxyapatite: Shape Transformation and Osteogenesis Activity", *Molecules* 2023, 28, 7379. <https://doi.org/10.3390/molecules28217379>
- [9] *Fatih Kurtuldu, Nurshen Muthu, Aldo R. Boccaccini, Dušan Galusek*, "Gallium containing bioactive materials: A review of anticancer, antibacterial, and osteogenic properties", *Bioactive Materials* Volume 17, November 2022, Pages 125-146 17 (2022) 125–146, <https://doi.org/10.1016/j.bioactmat.2021.12.034>
- [10] *Íris Soares, Lamborghini Sotelo, Ina Erceg, Florian Jean, Marie Lasgorceix, Anne Leriche, Maja Dutour Sikiric, Katarina Marušić, Silke Christiansen, Albena Daskalova*, Improvement of Metal-Doped β -TCP Scaffolds for Active Bone Substitutes via Ultra-Short Laser Structuring, *Bioengineering* 2023, 10, 1392. <https://doi.org/10.3390/bioengineering10121392>
- [11] *Rhianna McHendrie, Wenlong Xiao, Vi Khanh Truong, Reza Hashemi*, Gallium-Containing Materials and Their Potential within New-Generation Titanium Alloys for Biomedical Applications, *Biomimetics* 2023, 8, 573. <https://doi.org/10.3390/biomimetics8080573>
- [12] *Usanee Pantulap, Marcela Arango-Ospina, Aldo R. Boccaccini*, Bioactive glasses incorporating less-common ions to improve biological and physical properties, *Journal of Materials Science: Materials in Medicine* (2022) 33:3, <https://doi.org/10.1007/s10856-021-06626-3>